Resonant Scattering from Lightly Doped $La_{1-x}Sr_xMnO_3$ (x ~1/8) Single Crystals

K. Istomin, Y. Su, D. Hupfeld, A. Fattah, P. Foucart, T. Brückel
Institute of Solid State Research (IFF), Research Centre Jülich, Jülich, Germany

Introduction

Manganese oxides exhibit a rich variety of ground states whose interplay gives rise to many intriguing structural, electronic, and magnetic properties (e.g., colossal magnetoresistance). In spite of the intensive research carried out on these complex oxides in recent years, the underlying physics still remain largely unanswered [1].

In particular, in lightly doped $La_{1-x}Sr_xMnO_3$ (LSMO) ($0.1 < x < 0.15$) — one of most extensively studied manganites — the interplays among charge, orbital, spin, and lattice degrees of freedom are extremely complicated and remain a central issue with regard to the physics of manganites. Upon cooling down, lightly doped LSMO transforms from a paramagnetic insulating (PMI) state to a ferromagnetic metallic (FMM) state at the cure temperature (T_C). This FMM behavior can be understood in the framework of a double exchange model. An intriguing ferromagnetic insulating phase (PMI) appears further below T_C. To explain this insulating behavior, a charge/orbital-ordering scenario in PMI was proposed, which was then confirmed by the observation of orbital ordering via a resonant x-ray scattering (RXS) experiment on LSMO ($x = 0.12$) [2].

RXS has emerged as a powerful method to investigate the complex ordering phenomena in highly correlated electron systems. A number of successful measurements on transition-metal oxides have been carried out recently. However, the interpretation of the resonant scattering as a probe for orbital ordering is still open to debate [3, 4]. Some reports claim that the RXS is not a direct probe for orbital ordering (*OO*) but is much more sensitive to cooperative Jahn-Teller distortions and strongly coupled to band structure.

LSMO (x ~1/8) was then tipped as a unique model system to clarify this controversy, because it was believed that no Jahn-Teller distortions exist below T_{OO}. In fact, a long-accepted view of the structural aspects of lightly doped LSMO is that it possesses a pseudocubic symmetry above a Jahn-Teller transition temperature (T_J), then becomes a strongly Jahn-Teller-distorted orthorhombic phase below T_J, and finally goes back to a pseudocubic phase again below T_{OO} after a so-called reentrant phase transition. This simple image was recently questioned in a number of subsequent detailed structural characterizations and RXS measurements in a number of lightly doped LSMO samples [5-7], which indicated a much more complicated phase diagram [5] and identified a few novel structural phases with lower symmetry in the temperature range of orbital ordering [5, 6].

Methods and Materials

To clarify the controversial behaviors reported so far and to quantitatively evaluate the complex interplay among resonant scattering, orbital ordering, and structural effects (e.g., cooperative Jahn-Teller distortion and lower symmetry phases), a systematic approach has been undertaken to study a range of lightly doped LSMO ($0.1 < x < 0.15$) single crystals with a finely tuned Sr concentration x. In this report, preliminary results from resonant scattering on two x ~1/8 ($x = 0.125$ and $x = 0.135$) single-crystal samples are provided and briefly discussed. The powder rods were prepared by a standard solid-state synthesis process. Single crystals of LSMO ($0.1 < x < 0.15$) were grown in a mirror-image furnace by the floating-zone method. Crystals of excellent quality with cleaved (100) surfaces were obtained and then polished by diamond paste. The mosaic width of the (100) surface was determined to be less than 0.13° by the measurement of the rocking curve. The same crystals have been well characterized by electric and magnetic measurements, as shown in Figs. 1, 2(a), and 2(b). These samples have very sharp ferromagnetic transitions at T_C ~200K and ~210K, respectively. Below 200K, the resistance shows a small downturn, which is an indication of metallic behavior. A typical insulating feature appears again below about 140K.

The RXS measurements were undertaken at beamline 6-ID-B (Midwest Universities Collaborative Access Team [MU-CAT] sector) by using a standard four-circle vertical scattering geometry. The (100) plane of the sample was aligned within the scattering plane. A closed-cycle cryostat was used to cool down the sample. To discriminate the different polarization states of the scattered beam, a polarization analyzer setup was also employed.

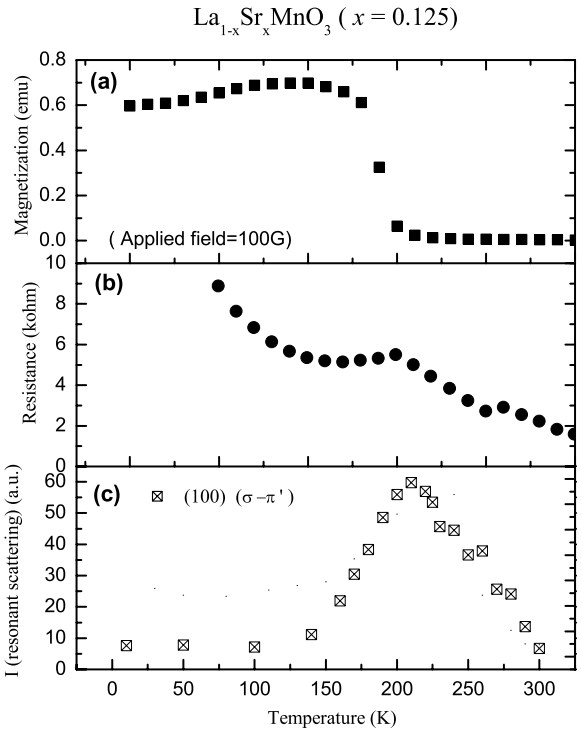

FIG. 1. Temperature behavior of magnetization (a), resistivity (b), and intensity of (1,0,0) reflection (c). x = 0.125.

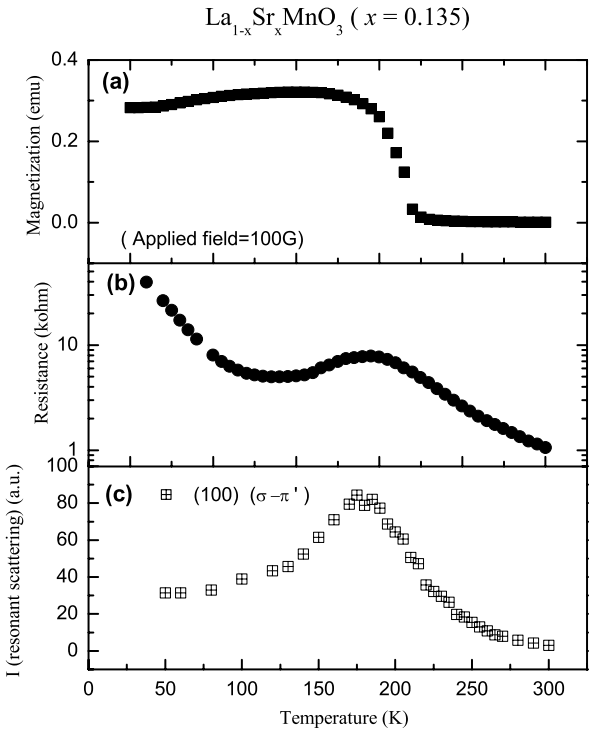

FIG. 2. Temperature behavior of magnetization (a), resistivity (b), and intensity of (1,0,0) reflection (c). x = 0.135.

Results

At room temperature, all Bragg reflections of the first sample (x = 0.125) are single peak along both longitudinal and transverse directions. Moving the sample surface around the incident beam indicates no peak splitting or multiple component. The other crystal (x = 0.135) has small grains, and the Bragg reflections demonstrate twinning.

When tuning incident x-ray energy close to the Mn K edge (see Fig. 3 inset), a huge resonant enhancement (by a factor of 20) from intensity of the forbidden reflection (1,0,0) was observed at E = 6555 eV. The energy dependence of (1,0,0) at 150K is shown in Fig. 3. Both samples have identical energy dependencies. The largest enhancement occurs around the white line of the absorption spectrum. Use of the polarization analyzer setup confirms that the scattered beam of (1,0,0) is predominantly $\sigma \rightarrow \pi$ scattered, which indicates a dipolar transition (1s $\rightarrow$ 4p)

Complete measurements of the temperature dependencies of resonant (1,0,0) scattering are shown in Figs. 1(c) (x = 0.125) and 2(c) (x = 0.135). The (1,0,0) resonance can even be observed at room temperature, a non-Jahn-Teller-distorted region. The intensity of the (1,0,0) resonant peak reaches a maximum at T = ~210K

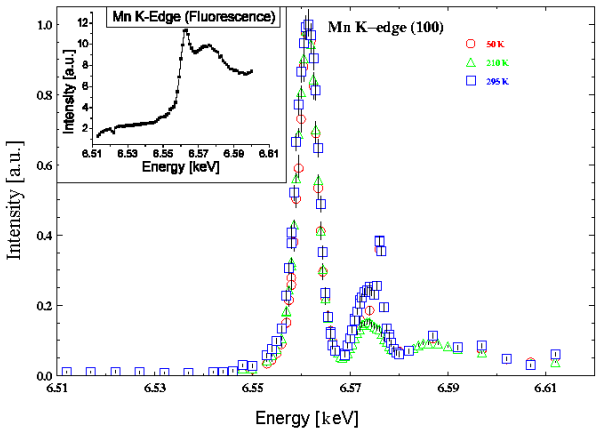

FIG. 3. Resonant enhancement of the forbidden (1,0,0) at the Mn K edge (x = 0.125 sample) at different temperatures normalized at the maximum. Inset: Fluorescence at T = 300K.

(x = 0.125) and T = ~180K (x = 0.135), then decreases upon cooling. Below T = ~120K, its intensity almost stays constant for both samples. Peak splittings along the longitudinal direction of the Bragg (2,0,0) reflection were

identified between 150 and 260K for $x = 0.125$ (between 120 and 230K for $x = 0.135$), where the (1,0,0) peak is split along transverse direction. Figure 4 shows the azimuthal scan obtained by rotating the crystal around the scattering vector kept at (1 0 0). The scan shows an almost sinusoidal-square angle dependence, but the intensities of the two maximas are different. This can be explained by a shading effect if the crystals are not perfectly oriented [i.e., the scattering surface of the crystal is not exactly (1 0 0) plane, but there is a miscut of a few degrees]. Experiments at the high-energy beamline 6-ID-D were performed with the same crystals. A large-area detector was placed behind the samples.

Figure 5 shows a typical pattern from the scattering of high-energy photons (88 keV) from the $x = 0.125$ sample. This pattern, which was obtained by rocking the sample $\pm 5°$ in the ϕ angle, shows the quality of crystal. Almost all Bragg reflections can be indexed, except for a few very weak ones that come from small grains of different orientation in the bulk of the crystal. These grains do not affect the RXS measurements when the scattering occurs in the upper-few-micrometer layer of the sample surface.

Discussion

We have observed strong resonant scattering at forbidden Bragg reflections, which is usually taken as an indication for orbital ordering in the lightly doped manganite samples. Further experiments are needed to correlate these findings with the temperature-dependent lattice distortions observed.

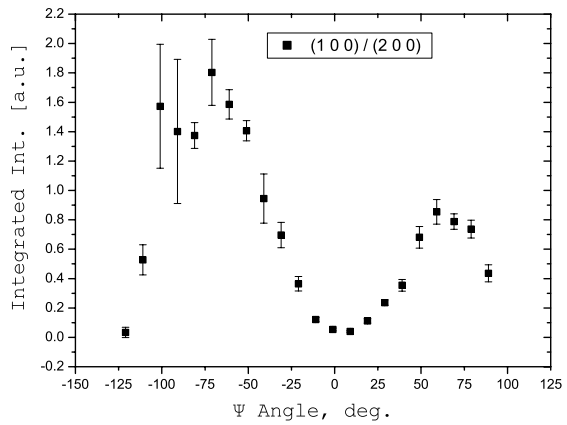

FIG. 4. Azimuthal dependence of the intensity of the (1,0,0) reflection normalized by the intensity of the (2,0,0) Bragg reflection. x = 0.135.

Acknowledgments

Use of the APS was supported by the U.S. Department of Energy (DOE), Office of Science, Office of Basic Energy Sciences (BES), under Contract No. W-31-109-ENG-38. The MU-CAT sector at the APS is supported by the DOE BES through Ames Laboratory under Contract No. W-7405-ENG-82. This work was supported by the German Federal Ministry of Education and Research under Contract No. 03-BR4DES-2.

References

[1] M. B. Salamon and M. Jaime, Rev. Mod. Phys. **73**, 583 (2001).
[2] Y. Endoh et al., Phys. Rev. Lett. **82**, 4328 (1999).
[3] M. Benfatto, Y. Joly and C. R. Natoli, Phys. Rev. Lett. **83**, 636 (1999).
[4] P. Benedetti et al., Phys. Rev. B **63**, 060408(R), (2001).
[5] D.E. Cox et al., Phys. Rev. B **64**, 024431 (2001).
[6] K. Tsuda et al., J. Phys. Soc. Jpn. **70**, 1010 (2001).
[7] J. Geck et al., Hasylab Annual Report (2000).
[8] Y.Su et al., Research Centre Jülich Annual Report (2001).

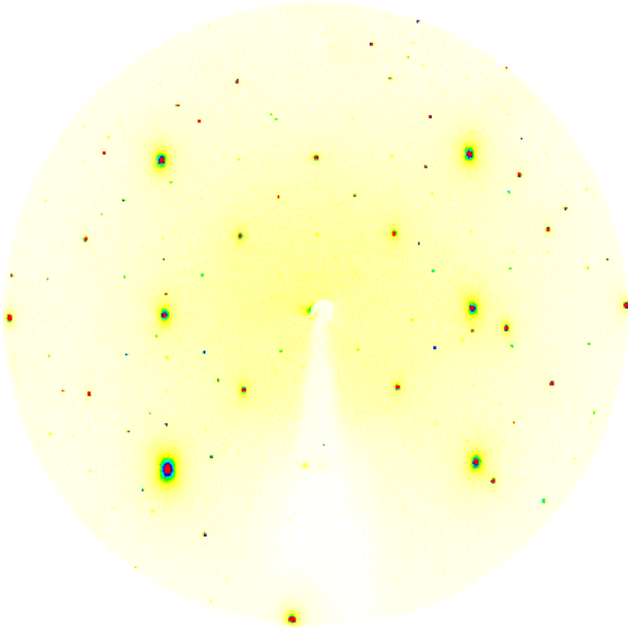

FIG. 5. High-energy pattern of the (h,k,0) plane of the x = 0.125 crystal. E = 88 keV and T = 300K.